Surface plasmon resonance and magnetism of thiol-capped gold nanoparticles

E Guerrero[1], M A Muñoz-Márquez[1]‡, M A García[2,3], P Crespo[2,3], E Fernández-Pinel[2], A Hernando[2,3] and A Fernández[1]

[1] Instituto de Ciencia de Materiales de Sevilla, CSIC-US, Av. Américo Vespucio 49, 41092-Sevilla, Spain

[2] Instituto de Magnetismo Aplicado (UCM-ADIF-CSIC), P.O. Box 155, 28230-Las Rozas, Madrid, Spain

[3] Departamento de Física de Materiales, UCM, 28040-Madrid, Spain

E-mail: `miguel.angel@icmse.csic.es`

Abstract. Surface plasmon resonance and magnetic characterization have been carried out for two types of thiol-capped gold nanoparticles (NPs) with similar diameters between 2.0 and 2.5 nm and different organic molecules linked to the sulphur atom: dodecanethiol and tiopronin. In addition, Au NPs capped with tetraoctyl ammonium bromide have also been included in the investigation since such capping molecules weakly interact with the gold surface atoms and, therefore, this system can be used as a model for naked gold NPs; such particles presented a bimodal size distribution with diameters around 1.5 and 5 nm. The plasmon resonance is non-existent for tiopronin-capped NPs, whereas a trace of such a feature is observed for NPs covered with dodecanethiol molecules and, a bulk-like feature is measured for NPs capped with tetralkyl ammonium salts. These differences would indicate that the modification of the surface electronic structure of the Au NPs depends on the geometry and self-assembling capabilities of the capping molecules and, on the electric charge transferred between Au and S atoms. Regarding the magnetization, dodecanethiol-capped NPs have a ferromagnetic-like behaviour, while the NPs capped with tiopronin exhibit a paramagnetic behaviour and tetralkyl ammonium-protected NPs are diamagnetic across the studied temperature range; straight chains with a well defined symmetry axis can induce orbital momentum on surface electrons close to the binding atoms. The orbital momentum not only contributes to the magnetization but also to the local anisotropy giving rise to permanent magnetism. Due to the domain structure of the adsorbed molecules, orbital momentum is not induced for tiopronin-capped NPs and the charge transfer only induces a paramagnetic spin component.

PACS numbers: 75.75.+a, 61.46.Df, 87.64.Fb, 73.20.Mf

Submitted to: *Nanotechnology*

‡ corresponding author

1. Introduction

The study of magnetic properties of Au clusters has drawn the attention of an important part of the scientific community since bulk gold is a non-magnetic system. In the past, self-assembled alkanethiol monolayers on gold surfaces have been reported to show permanent magnetism [1, 2] and, a more than plausible explanation of the magnetic properties has been proposed [3–6]. Such a magnetic behavior has also been observed in alkanethiol-capped gold nanoparticles, hereafter NPs, using a superconducting quantum interference device (SQUID) magnetometer [7, 8] and also by means of x-ray magnetic circular dichroism (XMCD) [9]. Unfortunately, despite all the experimental work, the magnetic properties of these nanoscale clusters are currently not well understood.

The high magnetic anisotropy required to block up the magnetic moment of Au NPs, with a diameter lower than 2 nm, up to room temperature suggests that orbital contribution to the magnetic moment can not be disregarded [6, 10]. The theory proposed by Hernando and co-workers [6], which reasonably explains the orbital magnetism observed in different nanostructured films, assumes the induction of orbital motion of surface electrons around ordered arrays of Au-S bonds. It is considered that electrons are pumped up from the substrate to the molecular layer [3], at the same time, spin-orbit effects, known to be extremely important in gold surfaces, must be taken into account; a strong spin-orbit coupling ($\alpha_r\hbar^2 = 0.4$ eV, were α_r is the splitting strength of the p band) has been measured for gold surfaces [11] by means of angle resolved photoemission spectroscopy and, theoretically described within a nearly-free-electron model [12]. Based on the latter statements, the L_z dependent part of the Hamiltonian H, were z stands for the direction normal to the surface plane, can be written as

$$H = \frac{L_z^2\hbar 2}{2m\xi^2} - \alpha_r L_z s_z \hbar^2, \tag{1}$$

here ξ is the radius of the thiol-capped region and, m and s_z are the mass and the spin component along the z axis of the free electron respectively. The value of the quantum number L_z that minimizes (1) is given by

$$L_z = m\xi^2\alpha_r s_z \tag{2}$$

This spin-orbit interaction together with a large radius of the self-assembled thiolated molecule domains should be the driving force for inducting orbital motion [6, 13].

Since gold NPs are most likely faceted clusters with an undetermined structure, the theory developed for two-dimensional systems could be extrapolated to Au NPs. It is to be noted that at least a fraction of the surface electrons have to keep their mobility or delocalization in order to be available for being captured in the orbits. In any case, regardless of what the details about the microscopic origins of the magnetization are, it seems to be well established that the magnetization arises from modifications of the NPs surface electronic structure biased by the binding between Au atoms and the organic molecules.

In order to obtain further experimental observations, we have carried out a systematic study of the microstructure, electronic properties, chemical composition

and magnetic behaviour on Au NPs. In this particular case, the gold clusters had approximately the same size and were functionalized with different organic molecules: i) dodecanethiol (H-S-$(CH_2)_{11}$-CH_3), ii) tiopronin (a thiol-containing biomolecule (H-S-$C_5H_8NO_3$) and iii) a tetralkyl ammonium salt (tetraoctyl ammonium bromide $BrN(C_8H_{17})_4$).

2. Experimental

2.1. Sample preparation

Dodecanethiol-capped gold NPs (Au-SR) were obtained from a liquid-liquid phase reduction at room temperature based on the Brust method [14], using a thiol:gold molar ratio of 2:1. First, Au(III) is transferred from an aqueous solution containing $HAuCl_4$ (FLUKA 99%, 0.064 g in 6.4 ml of milli-Q water) to degassed and dried toluene: tetraoctyl ammonium bromide (TOAB, Aldrich 98%, 0.112 g in 20 ml of toluene) is used as the phase-transfer agent. The mixture is strongly stirred for 10 minutes. Once the aqueous phase is removed, 0.1 ml of dodecanethiol are added to the organic phase under strong stirring for 5 minutes; the thiol was purchased from Aldrich and is 98.5% pure. Then, the formed Au-SR polymeric precursor is reduced with an aqueous solution of $NaBH_4$ (Aldrich 99%, 0.1 g in 6 ml of milli-Q water) which is a reducing agent. The presence of an alkanethiol leads to the formation of Au-S bonds which isolate the metal clusters preventing them from agglomeration. Subsequently, the organic phase was decanted from the aqueous phase and the toluene was removed under low pressure by means of a rotary evaporator. Finally, Au NPs were precipitated with ethanol, filtered, washed and dried.

Tiopronin-protected gold NPs (Au-ST) have been synthesized following the method developed by Templeton *et al.* [15], using a thiol:gold molar ratio of 1:1. The process will start by adding 0.060 g of tiopronin (Sigma) and 0.124 g of $HAuCl_4$ to a 14 ml 6:1 solution of methanol and acetic acid. Once this has been done, the solution turns into a red liquid. Then 0.24 g of reducing agent ($NaBH_4$ dissolved in 6 ml of milli-Q water) are added to the previous solution. The mixture is quickly stirred and turns immediately into a black suspension which will be stirred for 45 minutes. The next step is the solvent removal in low pressure by means of a rotary evaporator. Now, 25 ml of milli-Q water are added to the system and the acidity is corrected to pH=1 with concentrated HCl. The solution is then purified by dialyzis using cellulose membranes (Spectra/Por CE, MWCO=10000). The dialyzis process lasted 72 hours and milli-Q water was refilled every ten hours. Finally, water is removed by lyophilization.

The gold NPs protected with tetraoctyl ammonium bromide (Au-NR) were prepared following a modification of the method proposed by Reetz *et al.* [16]. This one-step redox-controlled size method consisted of the chemical reduction of the precursor salt using sodium borohydride as reducing agent in the presence of a stabilizer of the type $R_4N^+X^-$ which in our case is TOAB. The process will start by mixing two solutions:

one of 0.0112 g of TOAB in 150 ml of tetrahydrofuran (THF) and another one of 0.069 g of $HAuCl_4$ in 10 ml of THF. Once the final solution is ready, 0.006 g of $NaBH_4$ in 1 ml of methanol are added drop-by-drop. This will be followed by 30 minutes of strong stirring. Finally, the solvent is removed by means of a rotary evaporator.

2.2. Sample characterization

The iron and gold content in our samples was evaluated by inductively coupled plasma-atomic emission spectrometry analysis (ICP). The amount of light elements in the samples such as carbon, hydrogen, nitrogen and sulphur, was determined by elemental chemical analysis. The chemical composition of the samples was also measured by energy dispersive x-ray analysis (EDX) in the transmission electron microscope (TEM) mentioned next.

TEM analysis was carried out in a Philips CM200 microscope working at 200 kV. The approximate particle size distribution histograms were measured using an image analyzer software that determines the cluster radii from a digital image of the micrographs.

X-ray absorption spectra (XAS) of the Au samples were recorded in transmission mode at the BM29 beamline of ESRF. Spectra were recorded at the Au L_2- and L_3-edge, at 13734 and 11919 eV respectively. The extended x-ray absorption fine structure (EXAFS) oscillations were quantitatively analyzed with the software package developed by Bonin *et al.* [17]. The coordination numbers (N), bond distances (R) and Debye-Waller factors (σ) were extracted using a least-square fitting procedure that uses the theoretical phases and amplitudes proposed by Rehr and coworkers [18]. These parameters have been previously compared, for calibration purposes, to a pure gold foil and Au_2S (Aldrich, 99.9%) reference samples.

In order to study de surface plasmon resonance (SPR), UV-Vis absorption spectra were recorded in transmission mode. In these measurements, the gold NPs were dispersed in liquid solutions (1 mg/ml): the Au-SC_{12} sample was dissolved in toluene, the Au-ST NPs were dissolved in water and the Au-NR sample was dissolved in THF. The spectra were recorded in the range 200 to 850 nm with a Shimadzu UV-2102 PC spectrometer.

Magnetic measurements, at temperatures below 350 K, have been performed using a Quantum Design SQUID magnetometer. The sample holder is adhesive kapton which is sticked to a quartz tube. The diamagnetic contribution corresponding to the sample holder is previously measured and subtracted from the total magnetization.

3. Results and discussion

3.1. Structural and chemical characterization

Table 1 summarizes the chemical composition (as determined by ICP and elemental chemical analysis) and the NP average diameter (as determined by TEM) of the

investigated samples. Typical TEM images of these NPs can be found in previous publications [10, 19]. Regarding particle size and Au to S atomic ratio, both samples Au-SR and Au-ST are quite similar .

As it has been proposed in section 1, the gold NPs presented in this investigation are most likely faceted clusters. A comprehensive review by Yacamán *et al.* [20] has previously addressed this issue on the basis of a broad set of high resolution TEM (HRTEM) experiments. It is concluded that the capping agent, despite inducing a slight structure change, is responsible of the NP stabilization. Therefore, the structure of capped NPs would essentially be the same as the one of uncapped NPs. Experimental evidences are presented in [20] that would define gold NPs in the studied size range (1 - 5 nm) as truncated fcc cubo-octahedral clusters were the exact shape of the facets can not be univoquely determined.

Despite Au-S bonds are present in both dodecanethiol and tiopronin, there are significant differences concerning their spatial arrangement possibilities: whereas dodecanethiol chains are well known to self-assembly [21], the self-organization of tiopronin is not a straightforward issue. Recently, a normal incidence x-ray standing waves (NIXSW) structural study of adsorbed alkanethiols on a gold surface [22] has concluded that self-organization is determined by the relative strength of the intermolecular interactions and the lateral corrugation of the substrate potential. In particular, the corrugation of importance is the one associated to the Au-thiolate bonding in different sites. In the case of dodecanethiol, the intermolecular interactions may be strengthened by the linear geometry of the molecule, at the same time, due to the non-linear nature of tiopronin molecule, the aforementioned interactions will not be as strong as for linear dodecanethiol chains; figure 1 (bottom) shows a 'ball-stick' representation of both molecules. Considering the particular geometry of NPs and, the many different adsorption sites for thiolated species, the substrate potential corrugation will not play an important role in self-assembling. This would explain that self-assembly will not be favoured for tiopronin molecules. A schematic view of the two types of thiol-functionalization, in gold surfaces and Au NPs, is shown in figure 1. Regarding the tetralkyl ammonium salt, the interactions between the Au surface atoms and the protecting molecules are very weak indeed, therefore, no self-organized domains are formed.

3.2. Electronic structure and microstructure

In the XAS analysis of the samples both, the x-ray absorption near-edge structure (XANES) and the EXAFS oscillations were considered. However, a more detailed microstructural characterization of the samples can be extracted from figure 2 where the Fourier transform of the EXAFS oscillations of the Au L_3 XAS spectra are presented. This technique is very sensitive to the size and bond nature of the studied system, in this case gold NPs. In fact, the Fourier transform spectra of the Au-SR and Au-ST samples show both the Au-S and Au-Au coordination shell features, typical of thiol-

functionalized gold NPs. The Au-SR sample presents a stronger Au-S component as it is expected since the NPs of this sample have a slightly smaller diameter than the Au-ST NPs. The results of EXAFS simulations regarding coordination numbers and bond lengths are summarized in table 2 and are consistent with the slightly smaller particle size of the Au-SR samples. Data from the Au-NR sample correspond to a bimodal particle size distribution with nanoparticle diameters around 1.5 and 5 nm, as previously reported for the very same sample by TEM analysis [19].

Modifications of the electronic surface structure can also be detected through careful analysis of the SPR band in the UV-Vis absorption spectrum. It is well known that the capping process through Au-S bonds leads to a broadening of the SPR peak. Following the conclusions reported in a previous investigation [23], it would be expected that for a given particle size and density of surface bonds, the effective thickness where the electric charge is strongly localized can only be dependent on the bond nature; whilst for protecting molecules undergoing weak interaction the effective thickness should be zero.

According to the intensity of the experimental SPR band shown in figure 3, the electronic mobility of nanoparticle surface electrons is reduced dramatically when organic molecules are chemisorbed (through formation of localized Au-S bonds), as compared to weak-interacting protective organic molecules. However, also in NPs, the strong tendency to self-assembly could give rise to locally ordered islands of a few atoms (c.f. scheme in figure 1) [24]. The probability of ordered arrangement falls down when the geometry and composition of the protective molecules do not promote self-assembly interactions. Disorder in the Au-thiolate bonding arrangement is related with surface potential fluctuations that preclude collective motion of electrons decreasing the mobility and damping the SPR feature in the Au-ST sample as compared to the Au-SR one. At this point, it should be emphasized that the white line intensity at the Au L_2-edge (near edge structure) is exactly the same for both, the Au-ST and the Au-SR samples and slightly higher than the one corresponding to bulk gold. This would mean that there is a similar charge transfer at the localized Au-S bond for both samples [25] which would reinforce the argument regarding the self-organization. However, the Fourier transform of the EXAFS spectra indicates that the Au-ST sample has a smaller number of Au-S bonds and, therefore, the possibility of having a larger charge transfer at the Au-S bonds of the Au-ST sample, not detected through the white line intensity, remains open. In addition to the later possibility, the decrease of the SPR intensity of tiopronin-capped NPs when compared with the Au-SR sample has already been reported [15, 26] and a relation with the dielectric properties of the capping system is not completely clear.

3.3. Magnetic properties

Figure 4 depicts the differences in magnetic behaviour exhibited by the NPs, according to the nature of the capping molecules. For Au-SR NPs, the field dependence of magnetization is typical of ferromagnetic samples. Hysteresis loops recorded at 5 and

300 K indicate that magnetic moments are blocked at both temperatures; note that superparamagnetic features are not observed. For NPs with radius smaller than 3 nm, the anisotropy constant required to keep the magnetic moment blocked up should be as high as 10^8 Jm^{-3}. This value is extremely large and has been tentatively justified by considering spin-orbit coupling between the localized spin -associated with the hole created through charge transfer at the binding Au atom- and the angular momentum induced, around this atom, in conduction electrons [6]. The angular momentum can be induced and characterized by a well defined quantum number provided that the binding molecule is a symmetry axis as concerns its electrostatic potential on the surface of the Au NPs [6].

In contrast with the aforementioned behaviour, the magnetization of the Au-ST NPs presents a paramagnetic behaviour at 5 and 300 K which indicates that the spins induced through binding to S atoms fluctuate in orientation.

Finally, the Au-NR does not show any paramagnetic characteristic and behaves as a diamagnetic sample, as is the case for bulk gold. From the Au L_3-edge XANES data, no noticeable charge transfer is observed as it has been previously reported [19].

The results presented in figure 4 clearly point out that the induction of magnetic moment in gold NPs has its origin in the formation of Au-S bonds [1, 8] which, through the assembly of ordered arrays and modifications in the electron mobility, can enhance the surface induced magnetism. The arising of magnetic moments is explained by the experimentally detected charge transfer between Au and S atoms. However, the existence of permanent atomic magnetic moments only predicts a paramagnetic behaviour. The difference between the ferromagnetic and the paramagnetic behaviour observed for Au-SR and Au-ST NPs respectively, should be a consequence of the different modifications induced, by a similar number of Au-S bonds, in the electronic properties of the Au surface which depend on the molecular chain linked to S atom and, probably, in the formation of small self-assembling domains of tiopronin; remember that orbital momentum L_z is proportional to the domain radius ξ which will be quite small due to the non-linear geometry and self-assembling capabilities of the tiopronin molecule. The ferromagnetic-like behaviour has been shown to require strong local anisotropy that keeps blocked the atomic magnetic moments against thermal fluctuations. It has been observed that Au-SR NPs exhibit high anisotropy and ferromagnetic-like character, whereas Au-ST NPs behave as paramagnetic.

4. Conclusions

Gold NPs protected with three different molecules have been studied in order to compare their structure, electronic properties and magnetic behaviour. In addition to the data presented in this work, previous publications [15] also communicated that for alkanethiol-functionalized gold NPs, with similar particle sizes and Au:S ratios, the SPR feature had a higher intensity than the corresponding SPR from tiopronin-functionalized NPs. The origin of this effect still remains unclear; despite having similar

charge transfer between Au and S atoms, such a difference in the SPR intensity could arise from variations in dielectric properties of alkanethiolate *vs* tiopronin monolayers [26]. Although another possible explanation would be that there is a charge transfer difference behind the SPR intensity decrease and XANES measurements are not sensitive enough to discern such a small variation. Regarding the magnetic properties, capping with dodecanethiol chains may lead to spin induction and anisotropy enhancement, presumably associated with the simultaneous induction of orbital momentum. The straight line topology of the dodecanethiol molecule, as well as its known tendency to self-assembly, could account for the axial symmetry character required to generate constant orbital momentum. In contrast, the lack of axial symmetry in the potential created by the non-linear tiopronin molecule would rule out the induction of orbital momentum and, consequently, the spin induced by charge transfer is then free to fluctuate thermally in a paramagnetic way.

Acknowledgments

We wish to acknowledge the support of the ESRF and BM29 beamline staff. Financial support from the Spanish MEC (NAN2004-09125-C07) and "Junta de Andalucía" (Project P06-FQM-02254, group TEP217) is also acknowledged. E. Guerrero thanks the Spanish MEC for financial support.

References

[1] Carmeli I, Leitus G, Naaman R, Reich S and Vager Z 2003 *J. Chem. Phys.* **118** 10372
[2] Reich S, Leitus G and Feldman Y 2006 *Appl. Phys. Lett.* **88** 222502
[3] Vager Z and Naaman R 2004 *Phys. Rev. Lett.* **92** 087205
[4] Hernando A and García M A 2006 *Phys. Rev. Lett.* **96** 029703
[5] Vager Z and Naaman R 2006 *Phys. Rev. Lett.* **96** 029704
[6] Hernando A, Crespo P and García M A 2006 *Phys. Rev. Lett.* **96** 057206
[7] Hori H, Teranishi T, Nakae Y, Seino Y, Miyake M and Yamada S 1999 *Phys. Lett.* A **263** 406
[8] Crespo P, Litrán R, Rojas T C, Multigner M, de la Fuente J M, Sánchez-López J C, García M A, Hernando A, Penadés S and Fernández A 2004 *Phys. Rev. Lett.* **93** 087204
[9] Negishi Y, Tsunoyama H, Suzuki M, Kawamura N, Matsushita M M, Maruyama K, Sugawara T, Yokoyama T and Tsukuda T 2006 *J. Am. Chem. Soc.* **128** 12034
[10] Guerrero E, Rojas T C, Multigner M, Crespo P, Muñoz-Márquez M A, García M A, Hernando A and Fernández A 2007 *Acta Mat.* **55** 1723
[11] LaShell S, McDougall B A and Jensen E 1996 *Phys. Rev. Lett.* **77** 3419
[12] Petersen L and Hedegard P 2000 *Surf. Sci.* **459** 49
[13] Hernando A, Crespo P, García M A, Fernández-Pinel E, de la Venta J, Fernández A and Penadés S 2006 *Phys. Rev.* B **74** 052403
[14] Brust M, Walker M, Bethell D, Schiffrin D J and Whyman R 1994 *J. Chem. Soc., Chem. Commun.* **7** 801
[15] Templeton A C, Chen S, Gross S M and Murray R W 1999 *Langmuir* **15** 66
[16] Reetz M T and Maase M 1999 *Adv. Mater.* **11** 773
[17] Bonin D, Kaiser P, Freitigny C and Desbarres J 1989 *Structures fines d'absorption des rayons X en chimie, 3* ed Dexpert H, Michalowizc A and Verdagner M (Paris: Societé Française de Chimie)
[18] Zabinsky S I, Rehr J J, Ankudinov A, Albers R C and Eller M J 1995 *Phys. Rev.* B **52** 2995
[19] López-Cartes C, Rojas T C, Litrán R, Martínez-Martínez D, de la Fuente J M, Penadés S and Fernández A 2005 *J. Phys. Chem.* B **109** 8761
[20] Yacamán M J, Ascencio J A, Liu H and Gardea-Torresdey J 2001 *J. Vac. Sci. Technol.* B **19** 1091
[21] Bain C D, Troughton E B, Tao Y T, Evall J, Whitesides G M and Nuzzo R G 1989 *J. Am. Chem. Soc.* **111** 321
[22] Yu M, Bovet N, Satterley C J, Lovelock K R J, Milligan P K, Jones R G, Woodruff D P and Dhanak V 2006 *Phys. Rev. Lett.* **97** 166102
[23] García M A, de la Venta J, Crespo P, Llopis J J, Penadés S, Fernández A and Hernando A 2005 *Phys. Rev.* B **72** 241403(R)
[24] Jackson A M, Myerson J W and Stellacci F 2004 *Nature Mater.* **3** 330
[25] Zhang P and Sham T K 2002 *Appl. Phys. Lett.* **81** 736
[26] Persson B N J 1993 *Surf. Sci.* **281** 153

Tables and table captions

Table 1. Average size and chemical composition data for the selected samples.

Sample	Au wt%	Fe wt%	S wt%	N wt%	C wt%	H wt%	Au:S (at. ratio)	Dm[a] (nm)
Au-SR	50.3	0.007	4.1	—	24.3	4.4	2.0	2.0
Au-ST	62.4	0.024	4.9	2.2	10.0	1.3	2.0	2.5
Au-NR[b]	41.4	< 0.030	—	1.2	32.0	5.7	—	1.5 - 5

[a] Average particle size as calculated from particle size distribution histograms.
[b] Sample Au-NR shows a bimodal size distribution at 1.5 and 5 nm.

Table 2. Best fitting parameters of the Au L_3-edge EXAFS oscillations of samples.

Sample	Elements[a]	N[b]	R(Å)[c] (±0.02 Å)	σ(Å)[d]	$\Delta\sigma^2 \times 10^{-3}$ (Å^2)
Au foil	$(\text{Au-Au})_m$	12	2.85	0.073 ± 0.015	
Au_2S	(Au-S)	1.9 ± 0.4	2.31	0.063 ± 0.013	
Au-SR	(Au-S)	0.75 ± 0.15	2.30	0.093 ± 0.019	
	$(\text{Au-Au})_m$	5.0 ± 1.0	2.77	0.078 ± 0.016	0.8
Au-ST	(Au-S)	0.48 ± 0.10	2.26	0.090 ± 0.018	
	$(\text{Au-Au})_m$	8.9 ± 1.8	2.80	0.089 ± 0.018	2.6
Au-NR	(Au-S)	1.9 ± 0.4	2.20	0.049 ± 0.010	
	$(\text{Au-Au})_m$	8.0 ± 1.6	2.84	0.086 ± 0.017	2.1

[a] Type of atoms in the coordination shell.
[b] Coordination number.
[c] Bond length.
[d] Debye-Waller factor.

Figure captions

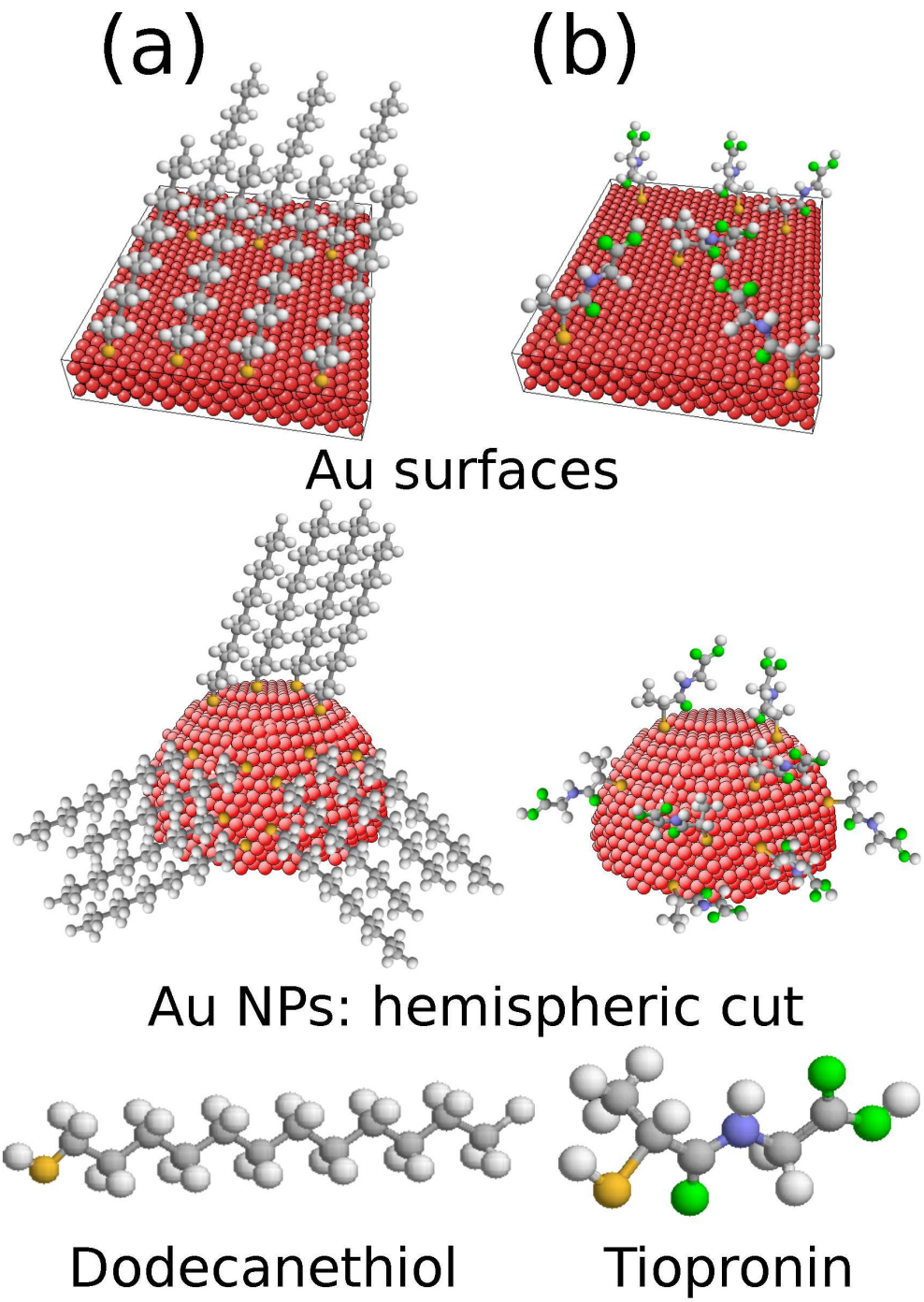

Figure 1. Scheme of self-assembled monolayer and non-ordered array formation: (a) for dodecanethiol- and, (b) for tiopronin-, functionalized gold surfaces and gold NPs: represented by a stacking model of red balls. The structure of the capping molecules is also shown using a 'ball-stick' model: hydrogen (white), carbon (grey), nitrogen (blue), oxygen (green) and sulphur (yellow).

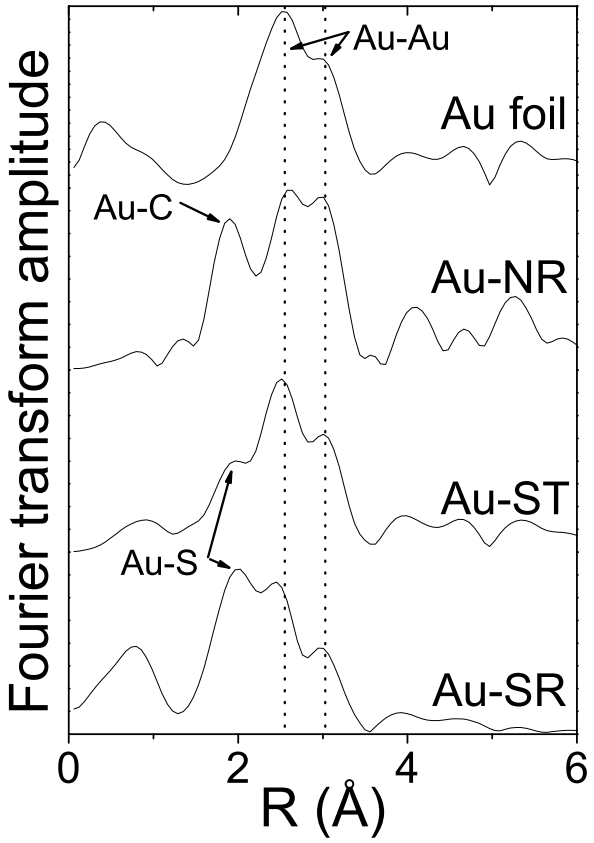

Figure 2. Modulus of the Fourier Transform of EXAFS oscillations at the Au-L_3-edge (k weighted, k space range of 2.8-13.2 Å^{-1} without phase corrections) for the Au-NR, Au-SR and Au-ST samples compared to bulk gold (Au foil) reference sample.

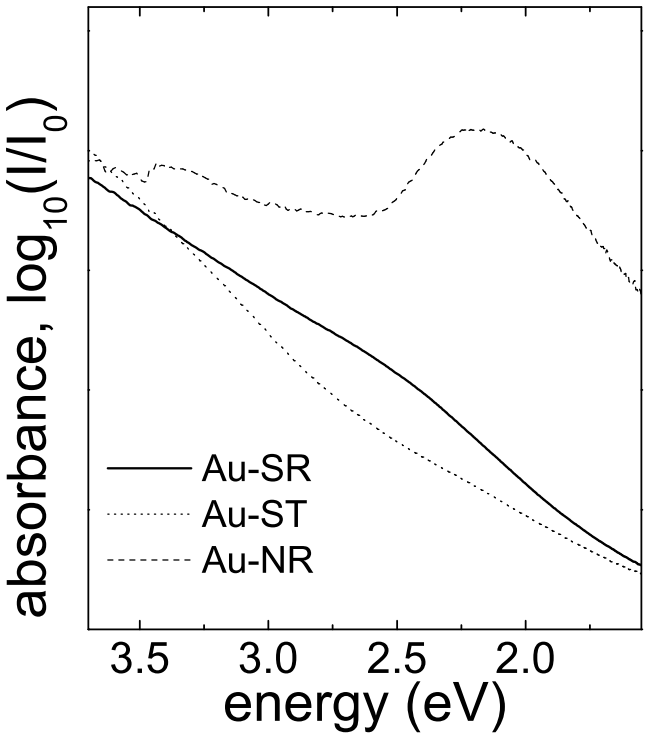

Figure 3. Optical absorption spectra from Au NPs with different capping systems.

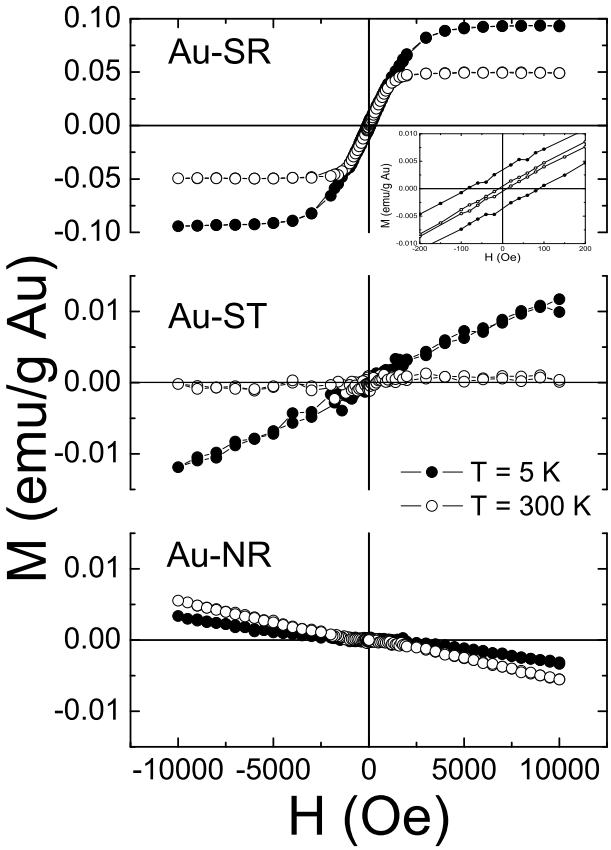

Figure 4. Hysteresis loops corresponding to the investigated gold NPs: Au-SR, Au-ST and Au-NR. Measurements were performed at two different temperatures: 5 and 300 K.